Structure and Dynamics of the Metal Site of Cadmium-Substituted Carboxypeptidase A in Solution and Crystalline States and under Steady-State Peptide Hydrolysis†

Rogert Bauer,*,‡ Eva Danielsen,‡ Lars Hemmingsen,‡ Marianne V. Sørensen,§ Jens Ulstrup,§ Esben P. Friis,§ David S. Auld,|| and Morten J. Bjerrum⊥

Department of Physics, The Royal Veterinary and Agricultural University, DK 1871 Frederiksberg C, Denmark, Department of Chemistry, Technical University of Denmark, 2800 Denmark, Center for Biochemical and Biophysical Sciences and Medicine and Department of Pathology, Harvard Medical School and Brigham and Women's Hospital, Boston, Massachusetts 02115, and Department of Chemistry, The Royal Veterinary and Agricultural University, DK 1871 Frederiksberg C, Denmark

Received April 22, 1997; Revised Manuscript Received July 8, 1997⊗

ABSTRACT: PAC spectra (perturbed angular correlation of γ-rays) of cadmium-substituted carboxypeptidase A (CPD) show that the enzyme in solution imposes a flexible, pH- and chloride-dependent coordination structure on the metal site, in contrast to what is found in the crystalline state. A much more restricted coordination geometry occurs for the steady-state peptide intermediates of Bz-Gly-L-Phe and Bz-Gly-Gly-L-Phe in solution, suggesting that substrate binding locks the structure in a rigid conformation. The results further indicate that the peptide intermediate has a six-coordinated metal coordination geometry with an OH^- ligand at the solvent site and a carbonyl oxygen at an additional ligand site. In marked contrast, conformational rigidity is not induced by the inhibitor/poor substrate Gly-L-Tyr nor by the products of high turnover substrates, Bz-Gly, Bz-Gly-Gly, and L-Phe. These results are consistent with an intact scissile peptide bond in the enzyme−substrate complex of Bz-Gly-L-Phe and Bz-Gly-Gly-L-Phe. A single nuclear quadrupole interaction (NQI) is observed for the crystalline state of the enzyme between pH 5.7 and pH 9.4. This NQI agrees with calculations based on the metal coordination geometry for cadmium in crystalline CPD derived from X-ray diffraction studies. A single broad distribution of NQIs is observed for CPD in sucrose solutions and 0.1 M NaCl at pH values below 6.5. This NQI (NQI-1′) has parameters very close to those for the crystalline state. The enzyme metal site, characterized by this NQI, is converted into two new enzyme metal sites over the pH range of 6.5−8.3. The metal coordination sphere of one of these has a NQI (NQI-1) with parameters similar to those at lower pH values (NQI-1′) while the other NQI (NQI-2) is characterized by markedly different NQI parameters. Angular overlap model (AOM) calculations indicate that the coordination sites giving NQI-1′ and NQI-1 both have a metal-bound water molecule while the coordination site giving NQI-2 has a metal-bound hydroxide ion. PAC results at pH 8.3−10.5 indicate that in this pH range the two metal coordination geometries related to NQI-1 and NQI-2 occur in a pH independent ratio of 2:1, with the one with the water ligand being the most abundant species. The observed pH-independent equilibrium between the two different metal coordination geometries for cadmium can be explained by an equilibrium between tautomeric forms of a hydrogen bond between the Glu-270 carboxyl group and the metal-bound water (Glu-270 $COO^-\cdots$(HOH)M ⇌ Glu-270 COOH$\cdots$(OH^-)M) being slow on the time scale of a PAC experiment, i.e., slower than 0.5 μs. We finally suggest that NQI-1′ observed at low pH reflects an enzyme species containing a metal-coordinated water molecule and the protonated carboxyl group of Glu-270.

Protein dynamics over broad time ranges (sub-picoseconds to seconds) are important in enzyme catalysis (*1*−*7*). Little attention, however, is given to protein dynamics in reaction mechanisms; the obvious reasons being that molecular details are quite elusive.

We have previously addressed enzyme dynamics by selecting peptide hydrolysis catalyzed by the Zn enzyme bovine carboxypeptidase A (CPD)[1] . CPD is structurally and kinetically well characterized. Hydrolysis of peptides represented by the dipeptide Bz-Gly-L-Phe is independent of the solvent viscosity η and has a small kinetic deuterium isotope effect (≈1.3) (*8*, *9*), in line with a rigid enzyme−substrate conformation. In contrast, Bz-Gly-L-OPhe ester hydrolysis has a larger isotope effect (≈2.5) and follows an exponential viscosity law ($\sim\eta^{-\delta}$; $\delta \approx 0.5$) indicative of strong conformational lability (*10*).

† The present work has been supported by the Danish Natural Research council via the Centre for Bioinorganic Chemistry.

* Correspondence to this author. Phone: 4535282307. Fax: 4535282350.

‡ Department of Physics, The Royal Veterinary and Agricultural University.

§ Technical University of Denmark.

|| Harvard Medical School and Brigham and Women's Hospital.

⊥ Department of Chemistry, The Royal Veterinary and Agricultural University.

⊗ Abstract published in *Advance ACS Abstracts,* September 1, 1997.

[1] Abbreviations: PAC, perturbed angular correlation of γ-rays; NQI, nuclear quadrupole interaction; AOM, angular overlap model; CPD, bovine carboxypeptidase A; Mrad/s, 10^6 radians per second; AAS, atomic absorption spectroscopy.

S0006-2960(97)00936-7 CCC: $14.00

In this study, we provide data for the flexibility of the enzyme and dynamics of the enzyme−peptide substrate interaction based on perturbed angular γ-ray correlation (PAC) spectroscopy of the Cd-substituted enzyme. This technique determines the nuclear quadrupole interaction (NQI) between a nucleus and its surrounding while in the intermediate state of a $\gamma-\gamma$ cascade. The isotope used is ^{111m}Cd, which decays to the ^{111}Cd ground state by successive emission of two γ-rays having a spin value of 5/2 in the intermediate state. The technique of perturbed angular correlations of γ-rays (PAC) is described in detail in the review by Frauenfelder and Steffen (*11*) and with special emphasis on biological applications by Bauer (*12*). In the presence of a NQI, the energy of the intermediate state is split into three different energy levels depending on the *z*-component of the 5/2 spin state. The energy differences ΔE_i ($i = 1, 2, 3$) are reflected in the measured PAC spectra as cosine oscillations with angular frequencies ω_i where $\Delta E_i = \omega_i h/2\pi$, *h* being Planck's constant. A given coordination geometry thus results in three peaks in the Fourier transform of a PAC spectrum at frequencies ω_1, ω_2, and ω_3.

The merit of ^{111m}Cd spectroscopy is the sensitivity to the structure of the metal site. In contrast to EXAFS, both the angular positions and the type of ligands can be obtained, and nanomole quantities are sufficient in data sampling. Conformational dynamics is also reflected in the bandshape features. Slow conformational changes (a time constant slower than 0.5 μs) affecting the metal coordination geometry produce broadening of the NQI, whereas conformational changes in the nanosecond regime affect the PAC spectra such that the dynamics of the process can be illuminated. Both structural and dynamic features can thus be derived from PAC spectra.

The present study first demonstrates that the Cd-CPD coordination geometry is only slightly different in the crystalline and solution states, except for an increased flexibility in solution. Secondly, pH- and anion-dependent equilibria between conformationally labile enzyme forms can be disentangled, suggestive of Cd(II) coordination to either water or hydroxide. Third, we demonstrate that the addition of the substrates Bz-Gly-L-Phe and Bz-Gly-Gly-L-Phe converts the enzyme to a conformationally much more rigid structure. This agrees with the insignificant viscosity effects on peptide hydrolysis. In contrast, PAC spectral data for Cd-CPD in the presence of the poor substrate Gly-L-Tyr are indicative of a poor match for catalysis between the enzyme and Gly-L-Tyr, reflected via a high conformational flexibility for the metal coordination geometry. For the substrates Bz-Gly-L-Phe and Bz-Gly-Gly-L-Phe, the coordination number is suggested to change from 5 to 6 for the peptide intermediates, having OH^- as a ligand at the solvent site and an additional carbonyl oxygen from the substrate as a sixth ligand.

MATERIALS AND METHODS

Reagents. Millipore water (Milli-Q Housing) and reagents of highest purity available were used. The substrate Bz-Gly-Gly-L-Phe was prepared as in Auld and Vallee (*13*), and the purity was checked by NMR spectroscopy. Where possible, laboratory utensils were made of polypropylene rather than glass and rinsed first in 10 mM 8-hydroxyquinoline-5-sulfonic acid and then in Milli-Q water. Salt and buffer solutions were normally purified by Chelex column chromatography (Chelex-100, 1 × 15 cm (Biorad)).

Carboxypeptidase A (CPD EC 3.4.17.1, Sigma type I) was purified by affinity chromatography. A HiTrap NHS-activated (*N*-hydroxysuccinimide ester) Sepharose column (Pharmacia), to which *p*-aminobenzyl succinic acid was coupled, was used, following the procedures in Bazzone et al. (*14*) and the recommendations from the manufacturer. The column was first equilibrated in 20 mM MES [2-(*N*-morpholino)ethanesulfonic acid] buffer containing 0.5 M NaCl (pH = 6). CPD dissolved in the same solution (8−10 mg mL^{-1}) was then injected and gradient eluted [buffer A: 50 mM Tris (Tris-hydroxymethyl)aminomethane, pH = 7.5; buffer B: 50 mM Tris, 0.5 M NaCl, pH = 7.5; 2 mL min^{-1}]. The main fraction, eluted around 0.25 M NaCl, was collected, ultrafiltrated (Amicon, YM5 membranes), and stored at 4 °C (50 mM Tris, 2 M NaCl, pH = 7.5). This procedure also applies to the Cd-substituted enzyme, whereas the apoenzyme does not bind to the affinity column.

The purified CPD was checked by UV spectroscopy ($\epsilon_{280} = 6.42 \times 10^4$ M^{-1} cm^{-1}), by atomic absorption spectroscopy (AAS) in the graphite furnace mode, and by activity assay toward the substrate Cbz-Gly-Gly-L-Phe [Cbz = carbobenzoxy, cf. Auld and Vallee (*13*)] using stopped-flow or conventional spectrophotometry (cf. below). AAS samples were 0.1 M in HNO_3. Both AAS and activity assays gave a 1:1 Zn:CPD ratio and 100% catalytic activity as compared to literature values, respectively.

Metal Substitution. Preparation of the apo- and Cd-substituted enzymes is critically sensitive to ubiquitous trace amounts of Zn. Metal substitution was therefore undertaken on CPD in the crystalline form (*15*). CPD (>5 mg mL^{-1}, 50 mM Tris, 2 M NaCl, pH = 7.5) was dialyzed in several steps against different buffers of decreasing ionic strength: (a) 50 mM Tris, 0.5 M NaCl, pH = 7 (1 h); (b) 25 mM Tris, 0.25 M NaCl, pH = 7 (1 h); (c) 12 mM Tris, 0.1 M NaCl, pH = 7 (1 h); (d) 5 mM Tris, 0.05 M NaCl, pH = 7 (overnight), and (e) 10 mM MES, pH = 7 (24 h). The small CPD crystals were centrifuged (5000 rpm), isolated, and stored in contact with 10 mM MES buffer at 4 °C. A total of 10−20 mg of CPD was incubated with 3−4 mL of aqueous 10 mM 1,10-phenanthroline and 10 mM MES (pH = 7) in a cryotube at 4 °C for 1 h with occasional stirring. This was followed by centrifugation at 4 °C, 5000 rpm for 10 min, and the supernatant was then replaced by a fresh solution. These steps were repeated three times. The crystals were rinsed five times with 3 mL of 10 mM MES (pH = 7) and stored in 0.3−0.4 mL of the same solution. An upper limit of 1.5 molar % of Zn was left by this procedure as detected by AAS. The apoenzyme could be reconstituted to about 95% activity by the addition of $Zn(NO_3)_2$ in 3-fold molar excess. Cross-linked crystals were made from apo-CPD crystals immersed in 0.02 M Veronal buffer pH 7.5 containing 1% glutaraldehyde for 2 h at room temperature. The cross-linked crystals were washed with 1 M NaCl and thereafter with 14 mM Tris-HCl, pH 9.

The procedure for preparation of the Cd-substituted enzyme followed that for the apoenzyme except that after rinsing the apoenzyme crystals two or three times with pure buffer, 10^{-3} M $Cd(NO_3)_2$ was added to the buffer. After removal of excess cadmium by rinsing the crystals with buffer at least twice, this gave more than 95% occupancy of

cadmium and less than 1% occupancy of zinc as detected by AAS.

Kinetic Measurements. Zn-CPD and Cd-CPD (10^{-4} M) catalyzed hydrolysis of Bz-Gly-L-Phe (Bz = benzoyl) was determined spectrophotometrically at 260 nm using $\Delta\epsilon_{260}$ = 280 M^{-1} cm^{-1} (*13*, *10*). The effect of anions on the activity of the Cd-substituted enzyme toward the dipeptide Bz-Gly-L-Phe substrate was investigated by stopped-flow spectrophotometry using a High-Tech SF.53 instrument combined with the OLIS (Jefferson, GA) data acquisition and processing software. The software tool "Grapher" from Golden Software inc. was used to process the initial rates vs substrate concentration.

The kinetics of Bz-Gly-Gly-L-Phe was followed by quenching the reaction mixture in 50 mM citrate, 10^{-3} M EDTA solution, or in glacial acetic acid, 10^{-3} M in EDTA. The quenched solutions were analyzed for L-Phe by HPLC. This analysis was carried out by Dr. V. Barkholt at the Department of Biochemistry and Nutrition at the Technical University of Denmark.

Cd-CPD has previously been reported to be inactive toward Bz-Gly-L-Phe but active toward Bz-Gly-Gly-L-Phe hydrolysis. The present investigations consistently show a Cd-CPD activity of approximately 6−7% (k_{cat}/K_M) of that for the native enzyme for Bz-Gly-L-Phe. This was unchanged by pre-equilibration of the solutions with 10^{-3} M $Cd(NO_3)_2$ over 24 h. Together with the much smaller upper limit for possible residual Zn (<1.5%, cf. above), these observations indicate that Cd-CPD does catalyze the hydrolysis of Bz-Gly-L-Phe.

PAC Sample Preparation. The ^{111m}Cd was delivered from the Cyclotron Department at the University Hospital in Copenhagen. A solution of 10−40 μL of $^{111m}Cd^{2+}$ containing about 10−40 pmol of $^{111}Cd^{2+}$ (no additional natural abundance of cadmium added) in H_2O was mixed with a volume from 40 to 100 μL of metal-depleted Tris-HCl (Tris free base + HCl) or MES buffer. Up to 50 μL of a suspension of apo-CPD crystals at a concentration from 0.5 to 3 mM was added, and the solution was left for 10 min at room temperature. In the sucrose experiments, sucrose was added to a final w/w concentration of 54%. pH was adjusted at room temperature by the addition of small amounts of 1−5 M HCl or NaOH. Within 10 min the sample was cooled to 1 ± 1 °C. The sample volumes were less than 50 μL in the crystal experiments and ranged from 200 to 1000 μL in the sucrose experiments. The apparent pH values given in this work were for all PAC experiments in 54% sucrose measured at room temperature immediately after the PAC spectra were recorded. For the PAC experiments in the crystalline state, the apparent pH values were measured at room temperature on the liquid withdrawn from the ^{111m}Cd-incubated crystals. The pH values for Tris and 55% sucrose at 1 °C can be obtained from the relation pH (1 °C) = 0.964 pH (25 °C) + 0.86 (*16*).

For the product and substrate PAC samples, sucrose was purified for traces of metal ions by using a Chelex-loaded column. The 10% sucrose solution in the appropriate buffer was purified, transferred to a rotor evaporator, and concentrated to 55% at 60 °C. This procedure reduced the reported $<5 \times 10^{-4}$ w/w % of Zn to about one-quarter of this value. All other PAC samples in sucrose were prepared under nitrogen atmosphere to exclude hydrogen carbonate. To avoid problems with extraneous metal ions, a 10 times higher CPD concentration was used. All manipulations, performed after the addition of the crystalline suspension of CPD, were carried out under nitrogen atmosphere and the sample sealed during PAC measurement. The PAC samples for experiments with CPD in the crystalline state (including cross-linked crystals) were handled under normal atmospheric condition and centrifuged to separate the crystalline phase.

PAC Spectroscopy. The PAC spectrometer consists of six BaF_2 scintillator detectors. Pairs of detectors form either 180° or 90° detector−sample−detector angles. The spectrometer is an extended version of the "PAC-camera" described previously (*17*). The temperature of the sample was controlled within 2 °C by a Peltier element. In total, six combinations with $\theta = 180°$ and 24 combinations with $\theta = 90°$ are collected simultaneously. The following so-called perturbation function is then constructed:

$$A_2G_2(t) = 2\frac{W(180°,t) - W(90°,t)}{W(180°,t) + 2W(90°,t)} \quad (1)$$

where $W(180°,t)$ denotes the geometric average of the 180° spectra, and $W(90°,t)$ is the geometric average of the 90° spectra. A_2 represents the anisotropy in the angular correlation, and $G_2(t)$ is the effect of a finite NQI. Before $G_2(t)$ can be derived, the $W(\theta,t)$ spectra must be corrected for a background due to accidental coincidences. Determination of the time resolution and zero point adjustment were performed with a ^{75}Se source. The time resolution is about 1 ns (full width at half maximum) at the energies of ^{111m}Cd. A non-vanishing NQI will split the intermediate state with spin 5/2 into three and not six sublevels because of the inversion symmetry of the NQI. In the case of identical, static, and randomly oriented molecules, the perturbation function $G_2(t)$ (eq 1) is

$$G_2(t) = a_0 + a_1 \cos(\omega_1 t) + a_2 \cos(\omega_2 t) + a_3 \cos(\omega_3 t) \quad (2)$$

where ω_1, ω_2, and ω_3 are the three difference frequencies between the three sublevels (*12*). Note that $\omega_1 + \omega_2 = \omega_3$.

Nuclear Quadrupole Interaction. The NQI is the interaction of the electric nuclear quadrupole moment of the nucleus (in the intermediate state) and the electric field gradient, V_{ij}, taken at the center of the nucleus where i,j refers to the Cartesian coordinate axis x, y, or z (*12*). Since the energy differences do not only depend on the electric field gradient but also on the value of the spin and nuclear quadrupole moment (Q) of the intermediate state of the nucleus, it is an advantage to relate the experimental results to the nuclear quadrupole interaction tensor:

$$\omega_{i,j} = \frac{12\pi|eQ|}{40h}V_{i,j} \quad (3)$$

where h is Planck's constant. For randomly oriented molecules, which applies to the present work, the orientation of the NQI tensor (eq 3) with respect to the protein cannot be determined. Thereby it is only possible to determine the diagonal elements of the tensor after diagonalization. Note that the sum $\omega_{xx} + \omega_{yy} + \omega_{zz}$ is equal to 0. The NQI is therefore parameterized by the largest diagonal element, $|\omega_{zz}|$, after diagonalization, and the asymmetry parameter. The two parameters obtained after diagonalization are

$$\omega_0 = |\omega_{zz}|$$
$$\eta = \left|\frac{\omega_{yy} - \omega_{xx}}{\omega_{zz}}\right| \quad (4)$$

The relation between these two parameters and the frequencies in eq 2 can be found in Bauer (*12*). Each frequency in eq 2 is proportional to $|\omega_{zz}|$ with a proportionality constant depending on η. The four amplitudes, a_0 ... a_3, also depend on η and sum to 1 in order to make $G_2(t) = 1$ for $t = 0$ to ensure full anisotropy. Thus from the time dependence of $G_2(t)$, $|\omega_{zz}|$ and η can be determined through least squares fitting.

Note that, only for $\eta = 0$, we have $\omega_0 = \omega_1$ where ω_1 is the first frequency in eq 2. For other values of η, ω_0 is monotonically decreasing from ω_1 to 0.567 ω_1 (value for $\eta = 1$).

In the present case, the nuclear quadrupole interaction can be time dependent in at least two ways. First, there is the reorientation of the protein and thereby of the electric field gradient caused by the rotational diffusion. This has the consequence that $G_2(t)$ converges to 0 as a function of time representing thermal equilibrium and isotropy in the angular correlation between the two γ-rays. The effect of rotational diffusion is described in Danielsen et al. (*18*). As the correlation time, τ_c, is much longer than $(\omega_0)^{-1}$ (see the tables), the dynamic perturbation function $G_2(t)$ can be expressed by modifying $G_2(t)$ by multiplying the right-hand side of eq 2 by $\exp(-t/\tau_c)$ (*19*). This will give rise to a Lorentzian line shape in the Fourier transformation of $G_2(t)$. A dynamic PAC spectrum will, secondly, appear if two (or more) coordination geometries are interconverted with a rate faster than 1/10th of the difference in the two corresponding ω_0 values.

PAC Data Analysis. The perturbation function $A_2G_2(t)$ was analyzed by a conventional non-linear least χ^2 fitting routine. The errors given in the tables are standard deviation and extracted from the error matrix and thereby include correlation between the parameters derived. For proteins, the peaks in the Fourier transform have never been as sharp as the limiting value, given by the spectral resolution of the experimental setup. Instead, the three frequencies observed in the Fourier transform of a PAC spectrum show broadening beyond the spectral resolution. In general, this can be fitted satisfactorily as a relative Gaussian distribution $\delta = \Delta\omega/\omega$ applied to all three frequencies. This is equivalent to a distribution in the values for ω_0 keeping η constant. The effect of δ (see below) and τ_c on the Fourier transform of a PAC spectrum can be seen in Figure 1. However, for some of the PAC spectra for ^{111m}Cd-carboxypeptidase, the second frequency is much broader than the first frequency. Such an effect has been observed for plastocyanin with Cu substituted by ^{111m}Cd and was shown to be related to movement in the plane perpendicular to ω_{yy} leaving ω_{yy} unchanged (*20*). Frequency broadening in this study is therefore accounted for by a relative Gaussian broadening of $\delta_1 = \Delta\omega_1/\omega_1$ and $\delta_2 = \Delta\omega_2/\omega_2$ for the first and second frequency, respectively. The distribution of the third sum frequency, ω_3, is set to $\Delta\omega_1 + \Delta\omega_2$. Finite values for δ_1 and δ_2 indicate that the ^{111m}Cd nuclei are located in a distribution of surroundings. A NQI is then described by the parameters ω_0, η, δ_1, δ_2, and τ_c.

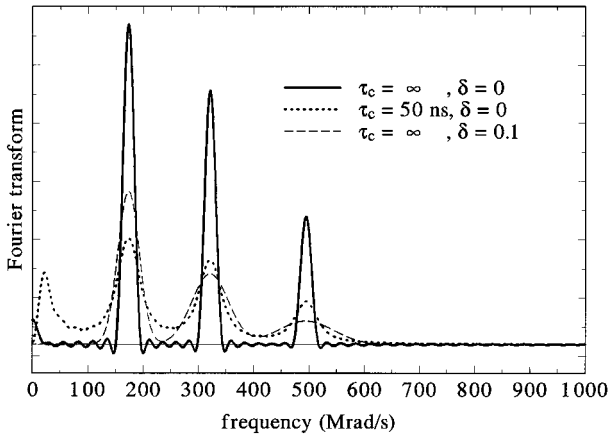

FIGURE 1: Fourier transform of theoretical PAC spectra with NQI parameters as NQI-1 at pH 10.5 (see Table 1). The frequency distribution is assumed to have $\delta_1 = \delta_2$. Note the peak close to zero frequency for $\tau_c = 50$ ns. It represents Lorentzian broadening of the frequency independent term a_0 in eq 2 and thus signifies rotational diffusion. All Fourier transforms in this work (theoretical end experimental) are cosine transforms. This is the natural choice as can be seen from eq 2.

In cases where more than a single NQI is present, the perturbation function is the sum of the different perturbation functions, where each NQI is weighted by its population. In the case of two different NQIs present simultaneously in a PAC spectrum, δ_1 and δ_2 separate into two values for each NQI, δ_{11} and δ_{21} for the first NQI and δ_{12} and δ_{22} for the second NQI.

Besides the determination of the NQI parameters δ_1 and δ_2, the value for τ_c is of interest for the dynamics/flexibility of the protein. As a reference point for τ_c, we use the NQI determined in 55% sucrose at 1 °C for alcohol dehydrogenase in the rigid ternary complex with NADH and DMSO (*21*). This NQI has a very low value for δ (here $\delta_1 = \delta_2$ was assumed), i.e., less than 0.01 and τ_c is equal to 400 ns. Scaling τ_c with the molar mass, we would have 175 ns for CPD in sucrose. Significantly smaller values of τ_c for CPD would indicate dynamic protein motion. Likewise, values larger than 0.01 for δ_1 and/or δ_2 would indicate protein flexibility on a time scale of 0.5 μs or slower.

Angular Overlap Model Calculations of NQI. In the interpretation of the measured NQIs, we have used the angular overlap model (AOM) in which the contribution to the electric field gradient from a specific ligand is assumed to be axially symmetric with respect to the ligand−metal bond direction, independent of the other ligands (*22*). Under these assumptions the independent contributions from different ligands, denoted partial NQI parameters, have been determined from model complexes (*22*). Thus, for example, a coordinating nitrogen in a histidine residue is assigned a unique partial NQI parameter. The partial nuclear quadrupole interactions of relevance here are (in 10^6 radians per second (Mrad/s)): carbonyl oxygen 161, monodentate carboxylate oxygen 245, bidentate carboxylate oxygen 175 each, water oxygen 207, and imidazole nitrogen 95. The partial NQI of a hydroxide ion has not been determined experimentally but is expected to be higher than that of water because of the additional charge. A PAC experiment on $Cd(OH)_2$ and *ab initio* calculations (Hemmingsen et al., unpublished result) suggests a value of 300 ± 50 Mrad/s. The NQI tensor can then be calculated as a sum over contributions from the different ligands:

$$\omega_{ij} = \frac{1}{2}\sum_{l}\omega_l(3\alpha_{il}\alpha_{jl} - \delta_{ij}) \quad (5)$$

where *ij* again refer to any of the three Cartesian coordinate axis *x*, *y*, and *z* centered at the metal ion, δ_{ij} is the delta Kronecker symbol, α_{jl} is one of the direction cosines, $\alpha_{xl} = \cos\phi_l \sin\theta_l$, $\alpha_{yl} = \sin\phi_l \sin\theta_l$, or $\alpha_{zl} = \cos\theta_l$, where θ_l and ϕ_l are the polar and azimuthal angles of the *l*th ligand and ω_l is the *l*th ligand's partial NQI parameter. ω_0 and η (see eq 4) are obtained by diagonalization of the tensor in eq 5.

NQI calculations applied to metalloproteins based on the AOM are treated in detail in Danielsen et al. (*23*) with special emphasis on a three-coordinated structure of two histidines and one cysteine. With typical experimental uncertainties, the technique is sensitive to changes in ligand−metal−ligand angles of only a few degrees. It is important to note that for a specific ligand differences in ligand−metal distance are ignored unless otherwise stated (*22*).

RESULTS

Kinetic Data. The values of the Michaelis−Menten constants k_{cat} (s^{-1}) and K_M (M) for the Cd-CPD catalyzed dipeptide Bz-Gly-L-Phe hydrolysis at 50 mM Tris, 0.5 M NaCl, 10^{-4}M Cd^{2+}, pH = 7.5 and 25 °C are 1.3 s^{-1} and 0.9 × 10^{-4} M, respectively. The corresponding values for Zn-CPD are 60−90 s^{-1} and 6−8 × 10^{-4} M, respectively, at 25 °C (*9*, *24*, *13*). The values for Cd-CPD catalyzed tripeptide Bz-Gly-Gly-L-Phe conversion are k_{cat} = 0.43 s^{-1} and K_M = 5.0 × 10^{-4} M, in comparison with the reported values of k_{cat} = 0.68 s^{-1} and K_M = 8.0 × 10^{-4} M for the cadmium enzyme (*25*) and k_{cat} = 20 s^{-1} and K_M = 8.0 × 10^{-4} M for the zinc enzyme (*13*).

Lowering the ionic strength from 0.5 to 0.1 M NaCl for the dipeptide hydrolysis raises k_{cat} to 1.7 s^{-1} and lowers K_M to 0.45 × 10^{-4} M for Cd-CPD. Changing the composition of the ionic medium from 0.5 M NaCl to 0.05 M NaCl + 0.45 M $NaClO_4$ (both with 50 mM Tris, 10^{-4} M Cd^{2+}, pH = 7.5) gives only minor changes in k_{cat} and K_M. The only significant change in kinetic parameters appears to be an increase in K_M with increasing ionic strength. Large concentrations of sucrose had no significant effect upon the carboxypeptidase catalyzed conversion of Bz-Gly-L-Phe (*26*, *9*).

PAC Data. Poor spectral resolution exists when PAC is applied to proteins having a molar mass of 30 000 or lower dissolved in solutions with the viscosity of water. This is caused by rotational diffusion of the protein which diminishes and broadens the three peaks in the Fourier transform through the factor $\exp(-t/\tau_c)$ (Figure 1). At 1 °C, τ_c is about 20 ns for a protein with mass 30000 g/mol. For this reason all PAC spectra reported here are either in 54% sucrose w/w, the crystalline state, or cross-linked in order to slow down rotational diffusion.

pH Behavior of NQIs from ^{111m}Cd-Carboxypeptidase A. PAC spectra of ^{111m}Cd-carboxypeptidase in solution as a function of pH are recorded at 1 °C, 54% sucrose and 0.1M NaCl (50 mM Tris or MES at pH values below 7). The Fourier transforms of the spectra at pH 5.6 and pH 10.5 are shown in Figure 2. Analysis of the individual spectra yields the NQIs shown in Table 1. Two NQIs are simultaneously present in all spectra above pH 6.5. These are denoted NQI-1 and NQI-2, the characteristic of NQI-1 being an ω_{01} value of about 160 Mrad/s and of NQI-2 being an ω_{02} value of about 200 Mrad/s. The spectral appearance of these two NQIs can be seen in Figure 2. The percentage of NQI-2 as a function of pH is given in Table 1. At pH values ≤6.5, NQI-2 is either absent or present to only a few percent. Furthermore, at these pH values, the NQI (here denoted NQI-1′, see Figure 2) has a broader distribution of NQIs than NQI-1 observed at higher pH values.

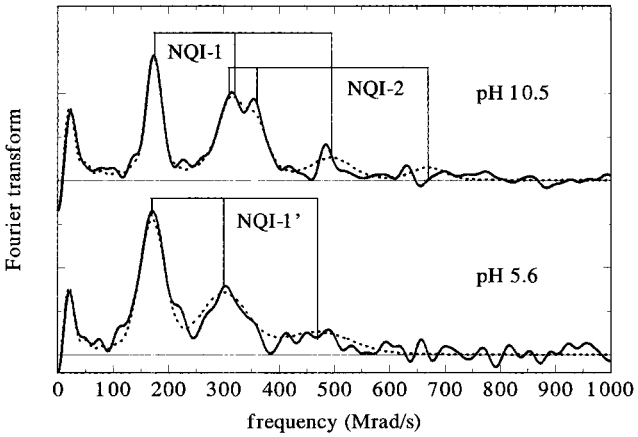

FIGURE 2: Fourier transform of PAC spectra from ^{111m}Cd-carboxypeptidase at pH 5.6 and pH 10.5 (54% sucrose, 0.1 M NaCl, 50 mM Tris-HCl, 1 °C). The solid lines represent Fourier transforms of the PAC spectra, and the dotted lines represent Fourier transforms of the least squares fits to the PAC spectra. Vertical connected lines indicate the positions of the three frequencies constituting each of the three derived NQIs. Noise in the Fourier transforms is random and centered around zero (horizontal solid lines) in regions where no NQI frequencies are observed.

The parameters corresponding to NQI-2 do not change significantly with pH while the ω_0 value increases from 154 Mrad/s at pH 5.6 for NQI-1′ to 163 Mrad/s at pH 10.5 for NQI-1 and η decreases from 0.32 at pH 5.6 to 0.25 at pH 10.5 (Table 1). This probably reflects the effect of ionizations of side chains of amino acids, such as the carboxyl group of Glu-270 at low pH and perhaps the phenolic group of Tyr-248 at high pH, that do not coordinate directly to the cadmium but still are closer than 6 Å from it. No significant variation of τ_c with pH is observed. Its average value is slightly lower than that predicted from alcohol dehydrogenase when corrected from the difference in molar mass (*21*).

NQI Dependence on NaCl Concentration and Physical State of ^{111m}Cd-Carboxypeptidase A. PAC spectra for the crystalline enzyme are obtained by adding $^{111m}Cd^{2+}$ ions to a crystalline apo-CPD suspension in less than 10 mM buffer. The results of the least squares minimization is given in Table 2. Only a single very narrowly distributed NQI is present (Table 2). This NQI has ω_0 and η values almost identical to the values for ω_{01} and η_1 observed in sucrose solution at pH 7.1 (Tables 1 and 2). The major difference being a much broader distribution of NQIs in solution (Tables 1 and 2 and Figure 3). A second difference is the absence or a very low content of NQI-2 in the crystalline state, except for cross-linked crystals at 1 M NaCl (Tables 2 and 3). No rotational diffusion of CPD is expected for the crystalline state on the time scale of nanoseconds, i.e., $\tau_c = \infty$. However, large but finite values for τ_c are found. This could indicate a dynamic interaction in the crystalline state, or it could represent a minor fraction of CPD dissolved. The latter suggestion is

Table 1: pH Dependence of NQI Parameters for ^{111m}Cd-Carboxypeptidase A[a]

pH	ω_{01}[b]	η_1	δ_{11}	δ_{21}	ω_{02}[b]	η_2	δ_{12}[c]	NQI-2 (%)	τ_c (ns)
5.6	154 ± 1	0.32 ± 0.02	0.11 ± 0.01	0.13 ± 0.01	200[d]	0.85[d]	0.05[d]	0 ± 2	147 ± 20
6.5	154 ± 1	0.33 ± 0.01	0.05 ± 0.01	0.10 ± 0.01	200[d]	0.85[d]	0.05[d]	2 ± 2	129 ± 13
7.1	156 ± 1	0.29 ± 0.02	0.03 ± 0.01	0.11 ± 0.01	200[d]	0.85[d]	0.05[d]	15 ± 3	119 ± 16
8.3	156 ± 1	0.28 ± 0.02	0.02 ± 0.01	0.10 ± 0.01	198 ± 1	0.86 ± 0.01	0.04 ± 0.01	33 ± 3	141 ± 14
9.3	160 ± 2	0.27 ± 0.03	0.03 ± 0.02	0.12 ± 0.02	200 ± 2	0.85 ± 0.01	0.05 ± 0.01	41 ± 3	121 ± 16
10.5	163 ± 2	0.25 ± 0.02	0.01 ± 0.03	0.10 ± 0.02	198 ± 2	0.83 ± 0.02	0.04 ± 0.01	32 ± 3	104 ± 11

[a] 20−40 μM CPD in 0.1 M NaCl, 54% sucrose at 1 °C in 50 mM MES (pH 5.6 and pH 6.5) or 50 mM Tris-base/Tris-HCl. [b] ω_0 values are in Mrad/s. [c] δ_{22} is set equal to δ_{12}. [d] Value fixed to that present at pH 9.3.

Table 2: NQIs in the Crystalline State of ^{111m}Cd-Carboxypeptidase A[a]

pH	ω_0 (Mrad/s)	η	δ_1	δ_2	τ_c (ns)	NQI-2 (%)[b]
5.7	156.9 ± 0.5	0.264 ± 0.003	0.007 ± 0.007	0.033 ± 0.002	249 ± 20	1 ± 3
7.5	158.4 ± 0.5	0.261 ± 0.004	0.003 ± 0.008	0.022 ± 0.002	313 ± 36	0 ± 3
8.6	157.9 ± 0.5	0.262 ± 0.003	0.012 ± 0.005	0.027 ± 0.002	535 ± 99	1 ± 3
9.4	158.1 ± 0.5	0.264 ± 0.004	0.002 ± 0.001	0.023 ± 0.002	376 ± 55	1 ± 3

[a] 4.2 mg of CPD in ≈50 μL of 9 mM MES (pH 5.7) and 1.4 mg of CPD in ≈50 μL of 5 mM Tris-HCl (all other pH values) at 1 °C. [b] The NQI parameters for NQI-2 are fixed at the values for cross-linked crystals in 1 M NaCl (see Table 3).

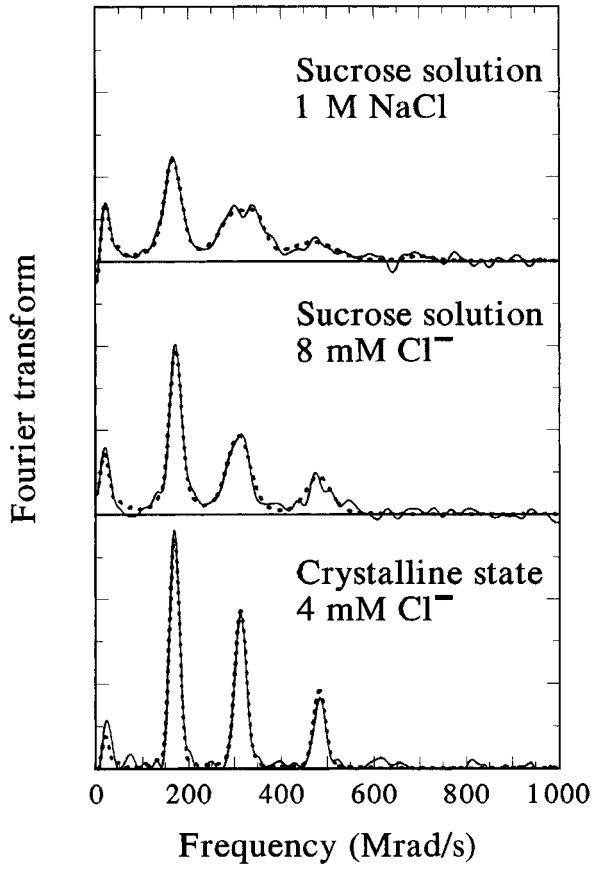

FIGURE 3: Fourier transform of PAC spectra in different physical states from ^{111m}Cd-carboxypeptidase A at pH 7.5. The solid and dotted lines are explained in the caption for Figure 2. The Cl^- concentration given in the figure comes from the titration of the Tris buffer with HCl. See Tables 2 and 3 for details.

unlikely because there is no evidence of the broad NQI observed in solution.

The NQI parameters in sucrose and 1 M NaCl pH 7.5 are almost identical to those found in sucrose and 0.1 M NaCl except for a slightly lower value of η for NQI-1 (Tables 1 and 3). Fourier transforms of PAC spectra for the crystalline state and the solution state with and without 1 M NaCl added are shown in Figure 3. Two PAC spectra are obtained with cross-linked crystals of CPD at pH 9 with and without 1 M NaCl. The Fourier transform of the PAC spectra is shown in Figure 4. The NQI parameters and conditions are given in Table 3.

NQIs for Peptide Intermediates and in the Presence of Peptide Products. PAC measurements are performed in the presence of about 50 mM Gly-L-Tyr, Bz-Gly-Gly-L-Phe, and Bz-Gly-L-Phe and the products Bz-Gly, Bz-Gly-Gly, and L-Phe in 54% sucrose and 0.1 M NaCl, pH 7.5. The amount of L-Phe is determined at the end of the PAC measurements for the two peptide experiments. 20 and 4 mM L-Phe are present for the dipeptide and tripeptide, respectively. This agrees with the faster rate of hydrolysis for the dipeptide relative to the tripeptide for the zinc enzymes (*24*, *25*) and the k_{cat} values found for the cadmium enzyme. The substrate concentration that remains at the end of the PAC experiments is still more than 10 times the K_M value for the substrate indicating that the concentration of the ES complex should be dominating during the experiments. The concentration of L-Phe, although higher than the inhibition constant (*27*), is still too low to compete effectively with substrate binding. The unique and sharp NQI found for the enzyme in the presence of the high turnover peptide substrates is very different from the NQIs found in the presence of any of the products (Table 4). From the above discussion it follows that product release is not the state before the rate-limiting step in Cd-CPD catalyzed hydrolysis of Bz-Gly-L-Phe and Bz-Gly-Gly-L-Phe. Chemical quenching studies of Zn- and Co-CPD catalyzed hydrolysis of peptides also indicate that the rate-limiting state is not product release (*28*, *29*). These results indicate that the Bz-Gly-L-Phe and Bz-Gly-Gly-L-Phe induced NQIs reflect the properties of the peptide intermediate and not those of a product complex.

Only a slight difference in ω_0 between the two protein-bound peptides is noted. The value of τ_c for the protein-bound dipeptide agrees with the value derived from alcohol dehydrogenase whereas the value for the protein-bound tripeptide is a factor of 2 lower. The latter observation could reflect a local dynamic effect in the nanosecond regime in catalysis which appears as rotational diffusion. The enzyme complexes of the products or the very low turnover substrate Gly-L-Tyr induce, on the other hand, insignificant shifts in ω_0 but substantial increases in both broadening and asym-

Table 3: Effect of the Anion Cl^- on the NQIs for ^{111m}Cd-Carboxypeptidase A

pH	condition[a]	ω_{01}[b]	η_1	δ_{11}	δ_{21}	ω_{02}[b]	η_2	δ_{12}[c]	NQI-2 (%)	τ_c (ns)
7.5	A	157 ± 1	0.31 ± 0.01	0.01 ± 0.01	0.06 ± 0.01	196[d]	0.84[d]	0.02[d]	1 ± 2	120 ± 8
7.5	B	160 ± 1	0.19 ± 0.02	0.07 ± 0.01	0.10 ± 0.02	194 ± 5	0.74 ± 0.08	0.05 ± 0.02	15 ± 2	98 ± 10
9.0	C	158 ± 1	0.28 ± 0.01	0.04 ± 0.01	0.07 ± 0.01	196 ± 1	0.84 ± 0.01	0.02 ± 0.04	14 ± 2	246 ± 34
9.0	D	158 ± 1	0.26 ± 0.01	0.06 ± 0.01	0.03 ± 0.01	189[e]	0.72[e]	0.04[e]	9 ± 4	756−∞
9.0	E	158 ± 1	0.22 ± 0.01	0.05 ± 0.01	0.04 ± 0.01	189 ± 1	0.72 ± 0.01	0.04 ± 0.01	26 ± 2	471 ± 97

[a] A, 30 μM CPD, pH 7.5, 54% sucrose; C, 90 μM CPD, pH 9.0, 49% sucrose both in 10 mM Tris-HCl; B, 30 μM CPD pH 7.5, 54% sucrose, 1 M NaCl in 50 mM Tris-HCl; D, 490 μM cross-linked CPD, pH 9.0 in 14 mM Tris-HCl; E, 490 μM cross-linked CPD, pH 9 in 50 mM Tris-HCl, 1 M NaCl. All experiments were performed at 1 °C. [b] Values in Mrad/s. [c] δ_{22} is set equal to δ_{12}. [d] Values fixed to that at condition C. [e] Values fixed to that at condition E.

Table 4: Substrate and product NQIs for ^{111m}Cd-carboxypeptidase A[a]

condition	ω_0 (Mrad/s)	η	δ_1	δ_2	τ_c (ns)
47 mM Bz-Gly-L-Phe	237 ± 1	0.15 ± 0.01	0.01 ± 0.01	0.02 ± 0.01	175 ± 22
47 mM Bz-Gly-Gly-L-Phe	241 ± 1	0.15 ± 0.01	0.04 ± 0.02	0.01 ± 0.01	94 ± 13
67 mM Gly-L-Tyr	155 ± 1	0.61 ± 0.01	0.09 ± 0.01	0.08 ± 0.01	152 ± 30
67 mM Bz-Gly (79 ± 4%)[b]	159 ± 2	0.30 ± 0.02	0.13 ± 0.01	0.12 ± 0.01	172 ± 21
67 mM Bz-Gly (21 ± 4%)[b]	167 ± 1	0.78 ± 0.01	0.02 ± 0.01	0.01 ± 0.02	172 ± 21
60 mM Bz-Gly-Gly	155 ± 2	0.35 ± 0.02	0.14 ± 0.01	0.15 ± 0.01	294 ± 52
60 mM L-Phe	116 ± 4	0.71 ± 0.06	0.10 ± 0.02	0.35 ± 0.05	74 ± 11
77 mM L-Phe (pH 10.0)	145 ± 1	0.39 ± 0.01	0.17 ± 0.01	0.12 ± 0.01	175 ± 21

[a] pH 7.5, 50 mM Tris-HCl, 54% sucrose, and 0.1 M NaCl. The concentration of CPD is 1 μM for the peptide substrates and Bz-Gly-Gly, but 0.4 μM for Bz-Gly and 20 μM for L-Phe. [b] Two NQIs are present with the given percent abundance.

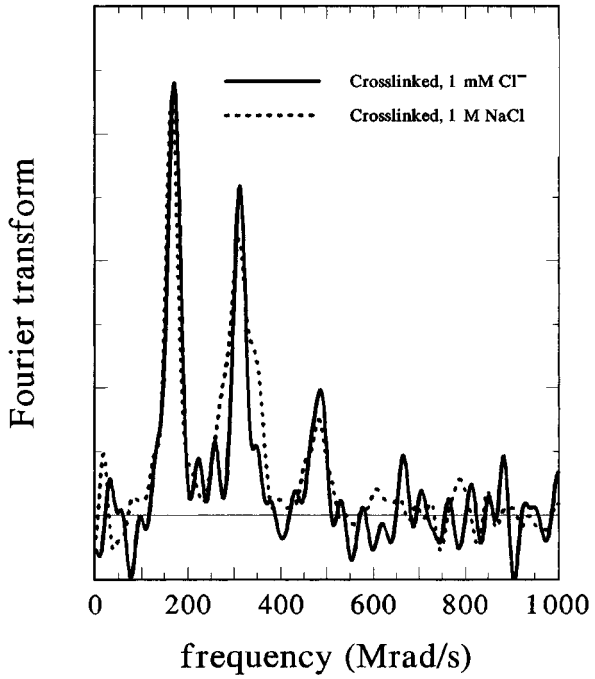

FIGURE 4: Fourier transform of PAC spectra from cross-linked crystals of ^{111m}Cd-carboxypeptidase A. The Cl^- concentration given in the figure comes from the titration of the Tris buffer with HCl. See Table 3 for details.

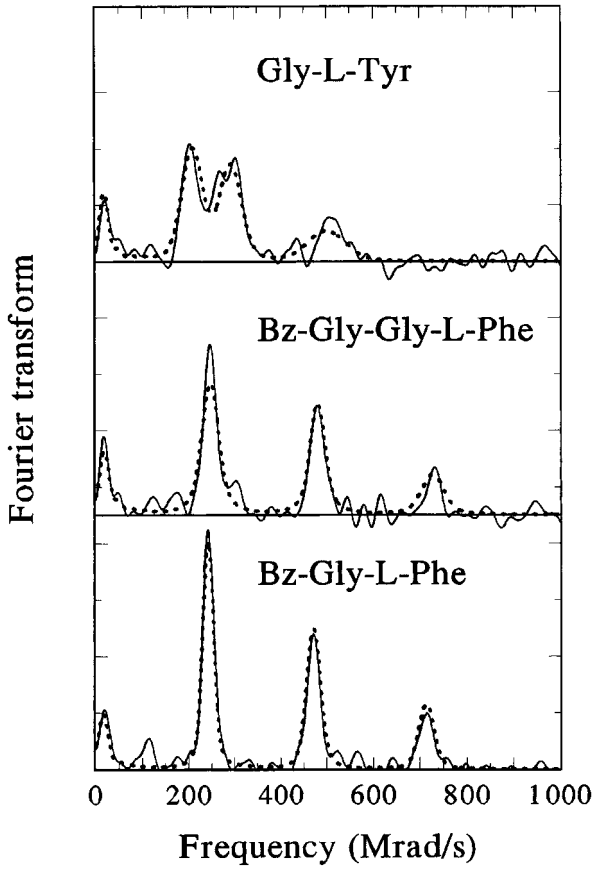

FIGURE 5: Fourier transform of PAC spectra in the presence of the three substrates. The solid and dotted lines are explained in the caption for Figure 2. See Table 4 for details.

metry parameters η relative to the NQIs for the free enzyme. This is indicative of notable conformational lability, in striking contrast to the apparent productive rigid structure induced by the good substrates. Fourier transforms of the PAC spectra for the high turnover peptides and Gly-L-Tyr are shown in Figure 5, and the Fourier transform of the three products are shown in Figures 6 and 7. The corresponding NQI parameters are given in Table 4.

The inhibitor L-Phe at pH 7.5 is unique in the sense that it produces the broadest NQI distribution observed (Figure 7 and Table 4). Furthermore, it also gives the lowest value of τ_c (Table 4). The change in the NQI in the presence of L-Phe at pH 7.5 could either be due to a contribution from the positive charge of the amino group in L-Phe, which then would have to be at a distance of about 4 Å from the cadmium ion (*30*), or a change in the angles of a few degrees of one of the ligands in the coordination sphere of Cd(II). At pH 10 the NQI in the presence of L-Phe is closer to NQI-1, and the distribution of NQI narrows (Figure 7 and Table

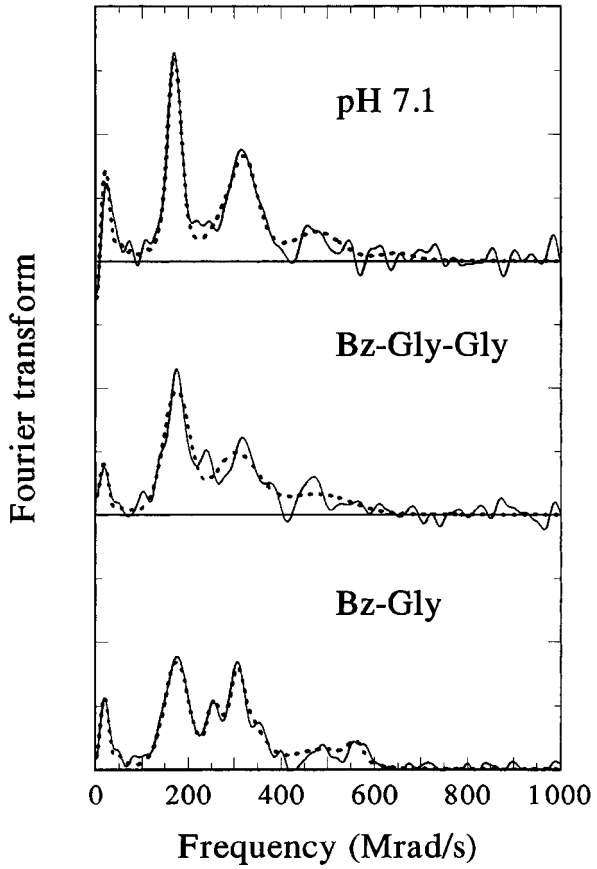

FIGURE 6: Fourier transform of PAC spectra in the presence of Bz-Gly, Bz-Gly-Gly, and the free enzyme at pH 7.1 for comparison. The solid and dotted lines are explained in the caption for Figure 2. See Tables 1 and 4 for details.

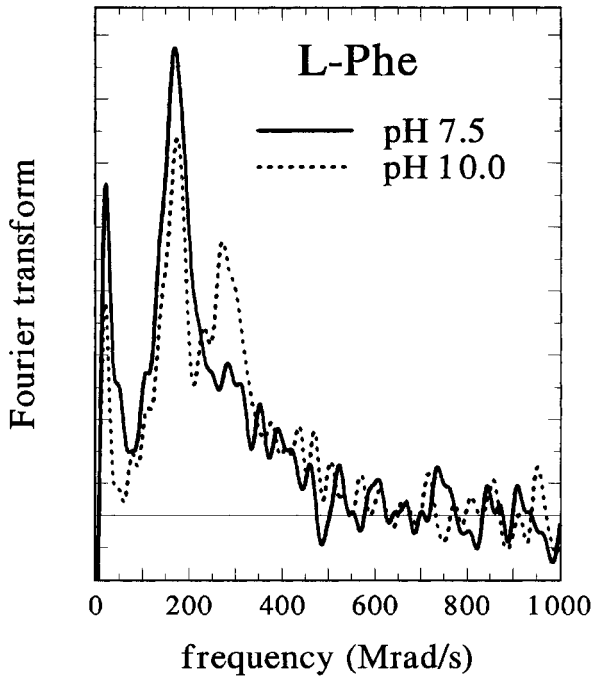

FIGURE 7: Fourier transform of PAC spectra in the presence of L-Phe at pH 7.5 and pH 10.0. See Table 4 for details.

4), although it is still much broader than without the inhibitor.

AOM Interpretations. The measured NQIs of carboxypeptidase A in the crystalline state and in solution are compared to AOM calculations based on the X-ray structure

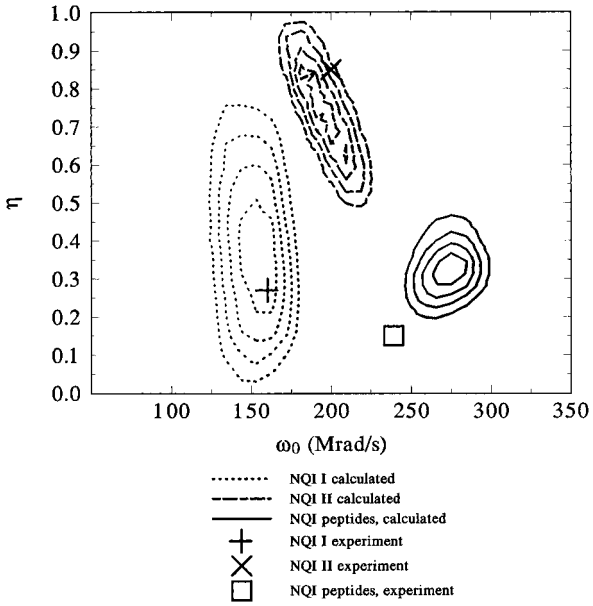

FIGURE 8: AOM calculations of NQIs represented as contour plots. The NQIs are calculated for angles in steps of 1° up to 5° for each ligand from their position derived from the X-ray structure of the cadmium enzyme (*31*) except that if a bidentate Glu-72 is included, only one of the coordinating oxygens angles is varied. The contour lines represent a constant level of probability for the occurrence of various values for ω_0 and η. The area inside the lowest contour level represents 95% of the area. The experimental values of the two NQIs for the dipeptide and tripeptide intermediate (Table 4) are average values. The calculations of NQI-1 and NQI-2 is performed with a water molecule and a hydroxide ion as the solvent ligand, respectively. The calculation of the NQI for the peptide intermediate is based on the six-coordinated structure mentioned in Table 5 having OH^- as the solvent ligand, but in addition having a sixth peptide carbonyl oxygen ligand.

of the cadmium enzyme (*31*). The AOM calculation yields an ω_0 of 150 Mrad/s and an η of 0.41. If the uncertainty in the X-ray data is taken into account, here assumed to be 5° in the angles of the ligands, the calculated values are in good accordance with the measured values of ω_0 and η, which are 158 Mrad/s and 0.26, respectively, in the crystalline state. Some selected experimental NQIs are shown in Figure 8. In Table 5, values of ω_0 and η are calculated using the five-coordinated geometry from X-ray diffraction data for the cadmium enzyme (*31*) having the two histidines, the bidentately coordinating carboxylate group of Glu-72 and either a water molecule, an OH^- ion, or a monodentately coordinating carboxylate ion at the solvent site as ligand. The NQI parameters for a four-coordinated geometry with water at the solvent site but changing the coordination of Glu-72 from bidentate to monodentate coordination are also calculated. Furthermore, ω_0 and η for various six-coordinated geometries with different ligands at the solvent site and different ligands in an additional position using the X-ray structure of the Gly-L-Tyr complex and CPD as the basis are also calculated (Protein Data Bank, Brookhaven National Laboratories, file: pdb3cpa).

The agreement between the experimental NQIs and those calculated by the AOM from the X-ray structure of cadmium carboxypeptidase A (*31*) is further illustrated in Figure 8 (see also Table 5). Figure 8 illustrates that neither NQI-2 present to about 35% in the spectra at high pH in solution (Table 1) nor the NQIs for the two peptide intermediates can be explained by changes within 5° in the angular position of

Table 5: AOM Calculated NQIs for ^{111m}Cd-Carboxypeptidase A[a]

complex	Glu-72	solvent ligand	6th ligand	ω_0 (exptl)	η (exptl)	ω_0 (calcd)	η (calcd)
crystalline state[b]	bidentate	H_2O	np[c]	158	0.26	150	0.41
solution state[d]	bidentate	OH^-	np	200	0.85	197	0.74
Bz-Gly[e]	bidentate	CO_2^-	np	167	0.78	169	0.46
peptide intermediate	monodentate	H_2O	np	239[f]	0.15	251	0.39
peptide intermediate	bidentate	H_2O	C=O	239[f]	0.15	225	0.98
peptide intermediate	bidentate	OH^-	C=O	239[f]	0.15	272	0.34
peptide intermediate	bidentate	H_2O	H_2O	239[f]	0.15	269	0.85
peptide intermediate	bidentate	H_2O	OH^-	239[f]	0.15	360	0.63

[a] All ω values in Mrad/s, the geometries are based on the structure for the cadmium enzyme (*31*) except for the sixth ligand position, which is derived from the X-ray structure of the Gly-L-Tyr complex (Protein Data Bank, Brookhaven National Laboratories, file: pdb3cpa). [b] Experimental NQI parameters from Table 2. [c] np, not present. [d] NQI parameters for NQI-2 (ω_{02} and η_2 at pH 9.3 from Table 1). [e] ω_0 and η are the NQI present to 21% in the PAC spectrum (Table 4). [f] Average of the ω_0 values for the two high turnover peptides (Table 4).

the water ligand for the free enzyme. For all three cases this is an indication of a change in the number and/or type of ligands. The contour plots in Figure 8 representing an OH^- metal ligand show that NQI-2 for cadmium carboxypeptidase A in solution at high pH can be explained by the ionization of a metal-coordinated water. The NQI of Bz-Gly present to about 20% in the PAC spectrum (Table 4) can similarly be explained by the substitution of the water ligand with a monodentate carboxylate oxygen (Table 5). In addition, it is clear from Figure 8 that the experimental point for the peptide intermediate falls in a separate NQI range. This range is not accessible by substitution of the solvent ligand by some other ligand. However, if Glu-72 only coordinates with one of its oxygen atoms resulting in a four-coordinated geometry (keeping water as the solvent ligand), the average of the two measured ω_0 values equal to 239 Mrad/s for the two high turnover peptides (Table 4) comes close to the calculated $\omega_0 = 251$ Mrad/s (Table 5). Another possibility is to increase the coordination number to six using the second solvent site observed in the Gly-L-Tyr complex for CPD as the sixth ligand position. The NQIs for various combinations of ligands at the first and second solvent site are then calculated (Table 5). Of these only OH^- at the first solvent site and a carbonyl oxygen at the second solvent site have calculated $\omega_0 = 271$ Mrad/s and $\eta = 0.34$ close to the experimental average values of $\omega_0 = 239$ Mrad/s and $\eta = 0.15$ (Table 5). In Figure 8, a contour plot for this solution is shown demonstrating that this solution as well as the four-coordinated structure with Glu-72 coordinating monodentately (Table 5) come close to the NQIs for the peptide intermediates. As can be seen in Figure 8 and Table 5, the six-coordinated solution has a 30 Mrad/s too high value for ω_0 as compared to the experimental values for the two peptides (Table 4). However, a peptide carbonyl connected to a metal ion in an intermediate state might not exhibit regular bonding. For this reason other values than 161 Mrad/s for the partial NQI for a carbonyl ligand were tried. The result was that changing the value for the partial NQI at the sixth ligand position from 161 Mrad/s to about 110 Mrad/s gives a calculated set of NQI parameters for the six-coordinated peptide intermediates, which fall within the uncertainty of the experimental values.

DISCUSSION

Effect of pH and NaCl Concentration upon NQIs for Cadmium Carboxypeptidase. One single well-defined NQI is observed in the crystalline state at 1 °C independent of pH (Table 2). A single broad NQI (NQI-1′) only slightly different from that observed in the crystalline state is detected by PAC in sucrose solutions at pH values below 6.5 (Figures 2 and 3 and Tables 1 and 2). At higher pH values, an NQI (NQI-1) very close in ω_0 and η to that derived at lower pH values is present to more than 50% (Table 1). From this, we conclude that the dominant coordination geometry in solution must be virtually identical to that in the crystalline state. AOM calculations indicate that this metal site contains a non-ionized water ligand (Table 5). However, the broad distribution observed in solution means that the crystalline state confines the coordination geometry and that the confinement is partly released in solution, resulting in a more flexible structure. The flexibility at low pH (5.6) can be described with $\delta_1 = \delta_2$, whereas a significant difference is found in δ_1 and δ_2 at higher pH values having $\delta_1 << \delta_2$. This behavior is typical of distributions in ligand positions restricted to a specific plane and has been observed for plastocyanin (*20*).

Another metal coordination geometry appears in solution at pH values higher than 6.5 and Cl^- concentrations ≥ 0.1 M. This NQI (NQI-2) reflects a metal geometry that reaches a maximum concentration by pH 8.3 representing about 35% of the metal species present (Table 1). AOM calculations indicate that this form of the metal site contains a metal-bound hydroxide (Table 5 and Figure 8). The absence of this species in the crystalline state could be partly due to the lower salt concentration used in the experiments but likely also because of crystal packing constraints. This follows from the PAC results at pH 9 in sucrose with 1 mM Cl^- (from HCl titration with Tris), where 14% of NQI-2 is still observed and from the PAC results with cross-linked crystals where 25% of NQI-2 is observed in 1 M NaCl (Table 3). Thus, at pH 9.4 in the crystalline state (less than 1 mM Cl^-) there should be a significant presence of NQI-2 if the sucrose solution mimics the crystalline state (Tables 2 and 3). The observed dependence of the concentration of NQI-2 on NaCl concentration (Figure 3 and Table 3) agrees with the finding of a partially competitive inhibitory site for low concentrations of Cl^- (*32*). The rigidity of the crystalline state, as reflected in the low values for δ, might prevent access for Cl^- to this site.

The Influence of the Ionization State of Glu-270 and Anions on the Metal Coordination Geometry for Cd(II)-CPD. The concentration of Cd-CPD with Cd(II) in the coordination geometry giving NQI-2 saturates at a presence of about 35% of the Cd sites. The two forms of Cd-CPD represented by NQI-1 and NQI-2 simultaneously present in solution with 0.1 M NaCl present and at pH 8.3, 9.3, and 10.5 must

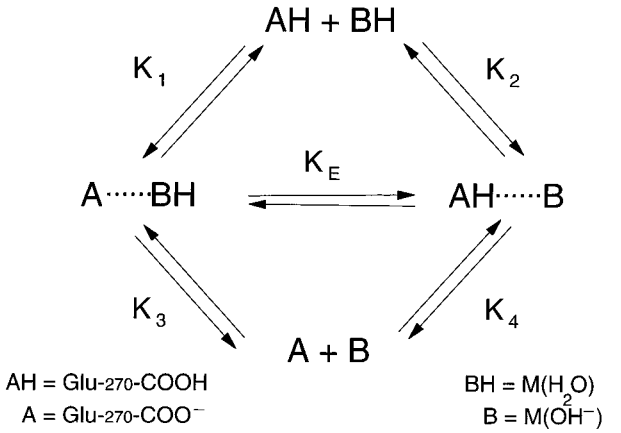

FIGURE 9: Proposed equilibria scheme consistent with the pH dependency of the NQIs from ^{111m}Cd-CPD in 0.1 M NaCl sucrose solution. The capital *K* values are dissociation constants, for example $K_1 = [H][A\cdots\cdots BH]/[AH + BH]$. From the corresponding four equations, it follows that $K_E = [A\cdots\cdots BH]/[AH\cdots\cdots B] = K_1/K_2 = K_4/K_3$. In the text, AH is proposed to be the protonated form of Glu-270, and BH is a metal-coordinated water molecule. Glu-270 is not proposed to coordinate directly to the metal, rather it is suggested to interact with the metal-coordinated H_2O or OH^- via a hydrogen bond.

therefore be directly connected via a pH-independent equilibrium. The simplest scheme of equilibria in line with this is given in Figure 9. The scheme can first be compared to the broadly applied view on the spectral and catalytic activity pH pattern for the Zn enzyme. Two pK_a values are associated with Zn-CPD structure and catalytic activity. The lower one (≈6) is most likely associated with the ionization of the carboxyl group of Glu-270 and subsequent H-bonding to the metal-bound water. The high pK_a (≈9) is suggested to be ionization of the metal-bound water ligand, based on recent NMR on Co-CPD (*33*) and EXAFS spectral data on ZnCPD (*34*, *35*). The pH dependence of the increase in concentration until saturation of the species reflected in NQI-2 for the Cd enzyme is indicative of a pK_a of about 7 (Table 1, 15% at pH 7.1 vs an average of 35% for the pH range 8.3−10.5). These results in conjunction with the additional broadening of the PAC spectra below pH 6.5 suggest that Glu-270 protonation and hydrogen bond breaking (between a metal coordinated water and the Glu-270 residue) could be a crucial physical element in the explanation of the decrease in k_{cat} observed for the zinc enzyme at low pH values (*36*). If the second pK_a, about 9 for the catalysis of the zinc enzyme, should be the release of the second proton in the hydrogen-bonded Glu-270 carboxylate and the coordinated water, then it must be much higher than 9 for the cadmium enzyme. This follows from Figure 9 and the assignment of a metal coordinated hydroxide ion to NQI-2, which then should reach a 100% presence in a PAC spectrum taken at pH values above pK_3 and pK_4 (Figure 9). In this respect, Cd-CPD follows observations for both carbonic anhydrase (*37*) and more recently alcohol dehydrogenase (*21*) where a shift in about two units upwards in the pK_a of a coordinated water molecule is observed. The lack of a second ionization for Cd(II)-CPD is paralleled by the situation for the Phe-248 mutant of carboxypeptidase where no change in K_M as a function of pH is observed (*38*).

The scheme in Figure 9 indicates why the observed 2:1 ratio between the presence of the species represented by NQI-1 and NQI-2 at pH 8.3 can occur. The microscopic equilibrium, K_E, between the Glu-270 $COO^-\cdots$(HOH)M and the Glu-270 $COOH\cdots(OH^-)$M species should be pH independent, and the ratio of their concentrations will be determined by the microscopic ionization constants $K_1/K_2 = K_4/K_3$. We propose that NQI-2 is assigned to a Cd^{2+} species to which OH^- is coordinated to the metal (Figure 9, species B) while the NQI-1 is related to a species that has a metal coordinated water molecule (Figure 9, species A) since these assignments are in agreement with the expected NQI parameters for a hydroxide and a water ligand, respectively (Table 5 and Figure 8). The equilibria (Figure 9) are based on two ionizing residues being so close to one another that interactions take place between them represented by the equilibrium constant K_E (Figure 9). This would imply that the pK_a of Glu-270 in Cd-CPD is shifted upwards by about one unit relative to ZnCPD (Table 1, 15% at pH 7.1 vs an average of 35% for the pH range 8.3−10.5). This could in principle be caused by differences in the polarization characteristics of Cd^{2+} and Zn^{2+}.

Interestingly, in the presence of L-Phe at high pH and 0.1 M NaCl, only one NQI is found (no presence of NQI-2) having ω_0 and η values close to those of NQI-1. At pH 7.5 and 0.1 M NaCl, again only one NQI is observed in the presence of L-Phe, but now quite different from NQI-1 and furthermore being very broad and with a very low value for τ_c. The broadness and the low value for τ_c indicate a very flexible protein with ligand movement in the nanosecond regime. In the presence of L-Phe there is thus no evidence for a pH-independent equilibrium such as that represented by K_E in Figure 9. The most obvious interpretation is that L-Phe breaks the hydrogen bond between metal coordinated water and Glu-270. The difference between pH 7.5 and pH 10.5 in the presence of L-Phe could be the ionization of the amino group in L-Phe that removes an additional positive charge close to the metal at pH 7.5. If this positive charge is at a distance of about 4 Å from Cd(II), it can explain the difference in the NQI values at low and high pH in the presence of L-Phe.

Metal Coordination Geometry for the Steady-State Peptide Intermediate. The spectra in Figure 5 and the NQI parameters in Table 4 show several intriguing differences from those corresponding to the free enzyme. The NQIs of the intermediate state in the presence of the high turnover substrates Bz-Gly-L-Phe and Bz-Gly-Gly-L-Phe are much sharper than the NQIs with no substrate present in solution. This is, interestingly, indicative of a more rigid enzyme conformation for the peptide intermediates than for the free enzyme and agrees with the lack of any significant viscosity effect for dipeptide catalysis (*9*). The NQIs of these two peptides are also shifted to higher values in ω_0 relative to NQI-1 for the free enzyme, and their positions in the contour plots shown in Figure 8 imply a change in the type, number, and/or angular positions of the metal ligands. There are two metal coordination geometries that by AOM calculations give NQIs close to those for the peptide intermediates (Table 5 and Figure 8): one six-coordinated metal geometry with the two histidines and a bidentately coordinating Glu-72, an OH^- ligand at the solvent site and a carbonyl oxygen at an additional ligand site, and one four-coordinated geometry with the two histidines, a monodentately coordinating Glu-72 and a water molecule as a solvent ligand. A monodentate Glu-72 metal coordination has been observed by X-ray diffraction studies of the potato inhibitor−carboxypeptidase

complex (*39*) and has been suggested for the ternary Zn and Co enzyme complexes of L-Phe and azide from EXAFS studies (*35*). However, the six-coordinated geometry would be expected for a peptide intermediate resulting from the abstraction of a proton from the metal-bound water by Glu-270 and the concurrent Lewis acid interaction of the metal ion with the peptide carbonyl (*40*).

Most strikingly, the slow substrate Gly-L-Tyr gives NQI parameters in the region of NQI-1 but far from those of the two N-terminal blocked (benzoylated derivatives) peptides (Tables 1 and 4). Furthermore, the NQI is broad for Gly-L-Tyr and close in value to the low pH NQI for the free enzyme. This indicates that Gly-L-Tyr is bound structurally different from the two N-terminal blocked peptides to the enzyme while in the steady-state complex.

The PAC spectral pattern of the enzyme−peptide substrate complex is in line with the complete absence of solvent viscosity effects on the native enzyme catalysis of Bz-Gly-Phe hydrolysis. Both the kinetics and the PAC spectral data are thus indicative of a structurally fairly rigid and well-defined enzyme−substrate complex. This is in striking contrast to Bz-Gly-OPhe ester hydrolysis. Strong viscosity effects on k_{cat} and a large kinetic deuterium isotope effect here point to a structurally "softer" and more flexible enzyme−substrate complex (*10*). This leads to notable damping of functional protein dynamics by the solvent. PAC spectroscopy may also hold clues to the molecular nature of these protein modes via the values for δ and τ_c.

ACKNOWLEDGMENT

The authors are indebted to Marianne Lund Jensen and Liselotte Jespersen for excellent help with sample preparations.

REFERENCES

1. Artymiuk, P. J., Blake, C. C. F., Grace, D. E. P., Oatley, J. J., Phillíps, D. C., and Sternberg, M. J. E. (1979) *Nature 280*, 563−568.
2. Frauenfelder, H., Petsko, G. A., and Tsernoglou, D. (1979) *Nature 280*, 558−563.
3. Friedman, J. M., Rousseau, D. L., and Ondrias, M. R. (1982) *Annu. Rev. Phys. Chem. 33*, 471−491.
4. McCammon, J. A., Wolynes, P., and Karplus, M. (1983) *Acc. Chem. Res. 16*, 187−193.
5. Gol'danskij, V. I., and Krupyanskij, Yu. F. (1989) *Q. Rev. Biophys. 22*, 39−92.
6. Welch, G. R. (1986) *The Fluctuating Enzyme*, Wiley, New York.
7. Sumi, H., and Ulstrup, J. (1988) *Biochim. Biophys. Acta 955*, 26−42.
8. Kaiser, B. L., and Kaiser, E. T. (1969) *Proc. Natl. Acad. Sci. U.S.A. 64*, 36−41.
9. Hammerstad-Pedersen, J. M., Khoshtariya, D. E., and Ulstrup, J. (1991) *Biochim. Biophys. Acta 1076*, 359−363.
10. Goguadze, N. G., Hammerstad-Pedersen, J. M., Khoshtariya, D. E., and Ulstrup, J. (1992) *Eur. J. Biochem. 200*, 423−429.
11. Frauenfelder, H., and Steffen, R. M. (1965) in *Alpha-Beta and Gamma-ray Spectroscopy* (Siegbahn, K., Ed.) pp 97−1198, Vol. 2, North-Holland, Amsterdam.
12. Bauer, R. (1985) *Q. Rev. Biophys. 18*, 1−64.
13. Auld, D. S., and Vallee, B. L. (1970) *Biochemistry 9*, 602−609.
14. Bazzone, T. J., Sokolovsky, M., Cueni, L. B., and Vallee, B. L. (1979) *Biochemistry 18*, 4362−4366.
15. Auld, D. S. (1988) *Methods Enzymol. 158*, 71−79.
16. Hemmingsen, L., Bauer, R., Bjerrum, M. J., Adolph, H. W., Zeppezauer, M., and Cedergren-Zeppezauer, E. (1996) *Eur. J. Biochem. 241*, 546−551.
17. Butz, T., Saibene, S., Fraenzke, T., and Weber, M. (1989) *Nucl. Instrum. Methods Phys. Res. Sect. A 284*, 417−421.
18. Danielsen, E., Bauer, R., and Schneider, D. (1991) *Eur. Biophys. J. 20*, 193−201.
19. Marshall, A. G., and Meares, C. F. (1972) *J. Chem. Phys. 56*, 1226−1229.
20. Tröger, W., Lippert, C., Butz, T., Sigfridsson, K., Hansson, O., Mclaughlin, E., Bauer, R., Danielsen, E., Hemmingsen, L., and Bjerrum M. J. (1996) *Z. Naturforsch. A51*, 431−436.
21. Hemmingsen, L., Bauer, R., Bjerrum, M. J., Zeppezauer, M., Adolph, H. W., Formicka, G., and Cedergren-Zeppezauer, E. (1995) *Biochemistry 34*, 7145−7153.
22. Bauer, R., Jensen, S. J., and Schmidt-Nielsen, B. (1988) *Hyperfine Interact. 39*, 203−234.
23. Danielsen, E., Bauer, R., Hemmingsen, L., Andersen, M., Bjerrum, M. J., Butz, T. E., Tröger, W., Karlsson, G., Canters, G., and Messerschmidt A. (1995) *J. Biol. Chem. 270*, 573−580.
24. Davies, R. C., Riordan, J. F., Auld, D. S., and Vallee, B. L. (1968) *Biochemistry 7*, 1090−1099.
25. Auld, D. S., and Holmquist, B. (1974) *Biochemistry 13*, 4355−4361.
26. Gavish, B., and Werber, M. M. (1979) *Biochemistry 18*, 1269−1275.
27. Auld, D. S., Larson, K., and Vallee, B. L. (1986) in *Zinc Enzymes*, (Bertini, I., Luchinat, C., Maret, W., and Zeppezauer, M.) Birkhauser, Boston. pp 133−154,
28. Galdes, A., Auld, D. S., and Vallee, B. L. (1986) *Biochemistry 25*, 646−651.
29. Geohegan, K. F., Galdes, A., Hanson, G., Holmquist, B., Auld, D. S., and Vallee, B. L. (1986) *Biochemistry 25*, 4669−4674.
30. Luchinat, C., Monnani, R., Roelens, S., Vallee, B. L., and Auld, D. S. (1988) *J. Inorg. Biochem. 32*, 1−6.
31. Rees, D. C., Howard, J. B., Chakrabarti, P., Yeates, T., Hsu, B. T., Hardman, K. D., and Lipscomb, W. N. (1986) in *Zinc Enzymes*, (Bertini, I. Luchinat, C. Maret, W., and Zeppezauer, M.) pp 155−165. Birkhauser, Boston.
32. Williams, A. C, and Auld, D. S. (1986) *Biochemistry 25*, 94−100.
33. Auld, D. S., Bertini, I., Donaire, A., Messori, L., and Moratal, J. M. (1992) *Biochemistry 31*, 3840−3846.
34. Zhang, K., and Auld, D. S. (1993) *Biochemistry 32*, 13844−13851.
35. Zhang, K., and Auld, D. S. (1995) *Biochemistry 34*, 16306−16312.
36. Auld, D. S., and Vallee, B. L. (1970) *Biochemistry 9*, 4352−4359.
37. Bauer, R., Limkilde, P., and Johansen, J. T. (1976) *Biochemistry 15*, 334−342.
38. Auld, D. S., Riordan, J. F., and Vallee, B. L. (1989) in *Metal Ions in Biological Systems* (Sigel, H., and Sigel, A., Eds.) Vol. 25, pp 359−394, Marcel and Dekker, Inc., New York and Basel.
39. Rees, D. C., and Lipscomb, W. N. (1982) *J. Mol. Biol. 160*, 475−498.
40. Auld, D. S. (1997) *Struct. Bonding 89*, 29−50.

BI970936T